
Replacing Rewards with Examples: Example-Based Policy Search via Recursive Classification

Benjamin Eysenbach^{1,2} Sergey Levine^{3,2} Ruslan Salakhutdinov¹

Abstract

In the standard Markov decision process formalism, users specify tasks by writing down a reward function. However, in many scenarios, the user is unable to describe the task in words or numbers, but can readily provide examples of what the world would look like if the task were solved. Motivated by this observation, we derive a control algorithm from first principles that aims to visit states that have a high probability of leading to successful outcomes, given only examples of successful outcome states. Prior work has approached similar problem settings in a two-stage process, first learning an auxiliary reward function and then optimizing this reward function using another reinforcement learning algorithm. In contrast, we derive a method based on recursive classification that eschews auxiliary reward functions and instead directly learns a value function from transitions and successful outcomes. Our method therefore requires fewer hyperparameters to tune and lines of code to debug. We show that our method satisfies a new data-driven Bellman equation, where examples take the place of the typical reward function term. Experiments show that our approach outperforms prior methods that learn explicit reward functions.

1. Introduction

In supervised learning settings, tasks are defined by data: what causes a car detector to detect cars is not the choice of loss function (which might be the same as for an airplane detector), but the choice of training data. Defining tasks in terms of data avoids manual engineering of objective functions, and is perhaps why supervised machine learning methods have been applied broadly to a wide range of domains. In contrast, reinforcement learning (RL) problems are typically posed in terms of a reward function, which

must be manually engineered. Arguably, the challenge of reward function design has limited the adoption of RL to applications where “success” can easily be described as a mathematical expression by users who speak this language of mathematically-defined reward functions. Can we make task specification in RL similarly “data-driven”?

Whereas the standard MDP formalism centers around predicting and maximizing the future reward, we will instead focus on the problem predicting whether a task will be solved in the future. The user will provide a collection of example success states, not a reward function. We will call this problem setting *example-based control*. In effect, these examples tell the agent “What would the world look like if the task were solved?” For example, for the task of opening a door, success examples correspond to different observations of the world when the door is open. The user can find examples of success even for tasks that they themselves do not know how to solve. For example, the user could solve the task using actions unavailable to the agent (e.g., the user may have two arms, but a robotic agent may have only one) or the user could find success examples by searching the internet. As we will discuss in Sec. 3.1, this problem setting is different from imitation learning: we maximize a different objective function and only assume access to success examples, not entire expert trajectories.

The key challenge in designing an algorithm to solve example-based control is identifying when the agent has solved the task and rewarding it for doing so. Prior methods for RL from data (either imitation learning from demonstrations or learning from success examples) use two-stage procedures that resemble inverse RL, first learning a separate model to represent the reward function, and then optimizing this reward function with standard RL algorithms. In contrast, we derive a method based on recursive classification that our method foregoes this separate reward learning stage; instead, we directly learn a value function from transitions and success examples (without any reward function). Our end-to-end approach removes potential biases in learning a separate reward function, reduces the number of hyperparameters, and simplifies the resulting implementation. We show that our method satisfies a new Bellman equation, where success examples are used in place of the standard

¹Carnegie Mellon University ²Google Brain ³UC Berkeley. Correspondence to: Benjamin Eysenbach <beysenba@cs.cmu.edu>.

reward function term. We use this result to provide convergence guarantees for the value function and policy.

This paper will also address a challenge in the formulation of example-based control: the probability that a particular state solves the task depends not only on whether the state was labeled as a success example, but also on the distribution used to select these success examples. Intuitively, some states might always solve the task while other states might rarely solve the task; without knowing how often the user visited each state, we cannot determine the likelihood that each state solves the task. Thus, an agent can only estimate the probability of success if they make an additional assumption about how the success examples were generated. This paper will discuss two choices of assumptions. The first choice of assumption is convenient from an algorithmic perspective, but sometimes violated in practice. A second choice is to resolve this ambiguity by taking a worst-case approach, a problem setting that we call *robust example-based control*. Our analysis shows that the robust example-based control objective is equivalent to minimizing the squared Hellinger distance (an f -divergence).

In summary, this paper studies a data-driven framing of control, where reward functions are replaced by examples of success, and the aim is to learn a policy that maximizes the probability of solving the task in the future. Our main contribution is an algorithm for off-policy example-based control. The key idea of the algorithm is to directly learn to predict whether the task will be solved in the future via *recursive classification*, without using separate reward learning and policy search procedures. Our analysis shows that our method satisfies a new Bellman equation where rewards are replaced by data (examples of success). Empirically, we demonstrate that our method excels at learning complex manipulation tasks solely from examples of success, outperforming prior two-stage approaches. On tasks with image observations, we demonstrate that the notion of success learned by our method generalizes to new environments with varying shapes and goal locations.

2. Related Work

Learning reward functions. Many prior works learn a reward function from data and then apply RL to this reward function. The learned reward function is often represented as a “success classifier,” which distinguishes successful outcomes from random states (Fu et al., 2018b; Singh et al., 2019; Zolna et al., 2020; Konyushkova et al., 2020). Recent work in this area focuses on extending these methods to the offline setting (Zolna et al., 2020; Konyushkova et al., 2020), incorporating additional sources of supervision (Zolna et al., 2019), and learning the classifier via positive-unlabeled classification (Xu & Denil, 2019; Irpan et al., 2019; Zolna et al., 2020). Many prior methods for robot learning have likewise

used a classifier to distinguish success examples (Calandra et al., 2017; Xie et al., 2018; Vecerik et al., 2019; Lu et al., 2020). Prior adversarial imitation learning methods (Ho & Ermon, 2016; Fu et al., 2018a) can be viewed as *iterated* versions of prior work on success classifiers. Whereas these imitation learning and success classifier methods focus on learning a policy, prior work on inverse RL (Pomerleau, 1989; Abbeel & Ng, 2004; Ratliff et al., 2006; Ziebart et al., 2008; Ross et al., 2011; Wulfmeier et al., 2015) aims to learn a reward function from expert trajectories. Unlike these prior methods, our approach only requires examples of successful outcomes (not expert trajectories) and does not learn a separate reward function. Instead, our method learns a value function directly from examples, without an intermediate learn reward function. Practically, this method removes all hyperparameters and avoids any potential bugs associated with learning a success classifier. Empirically, we demonstrate that our end-to-end approach outperforms these prior two-stage approaches.

Imitation learning without auxiliary classifiers. While example-based control is different from imitation learning, our method is related to two prior imitation learning methods that eschew an auxiliary reward function. Our method is similar to ValueDICE (Kostrikov et al., 2019) and SQIL (Reddy et al., 2020) in that we learn a value function directly from success examples. Like ValueDICE, our derivation makes use of an identity relating the state occupancy measure at consecutive time steps. Whereas ValueDICE uses this identity together with duality to minimize a KL divergence imitation learning objective, our derivation uses this identity to derive a method that maximizes the probability of future success. While our method bears a resemblance to SQIL, our derivation is based on a principled approach to example-based control, whereas SQIL is derived as an imitation learning method inspired by behavior cloning. Empirically, our method outperforms SQIL. Our analysis in Sec. 4.2 highlights connections and differences between imitation learning and example-based control.

Goal-conditioned RL. Example-based control is similar to goal-conditioned RL, which likewise can be viewed as maximizing the probability density of reaching certain states. In discrete state spaces, the value functions learned by goal-conditioned Q-learning (Sutton, 1995; Schaul et al., 2015) and successor features (Dayan, 1993; Kulkarni et al., 2016; Barreto et al., 2017) corresponds to the probability of reaching a certain state in the future. The most similar prior work is C-learning (Eysenbach et al., 2021), which shows how a similar bootstrapping procedure can be used to estimate the *density* of future states in continuous state spaces. While our derivation is largely inspired by C-learning, our method allows the agent to complete tasks that are more general than goal-reaching. As we will show in our experiments, the user

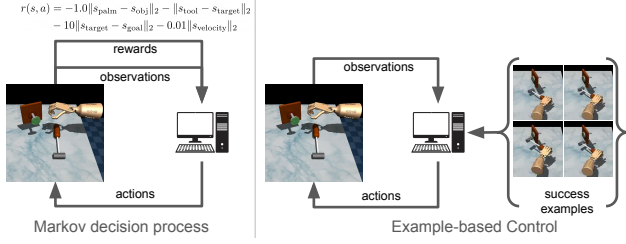


Figure 1. Example-based control: Whereas the standard MDP framework specifies requires a user-defined reward function, example-based control specifies tasks via a handful of user-provided success examples.

can indicate that tasks can be solved in many ways, allowing the agent to learn a more general notion of success. Unlike goal-conditioned RL methods, we aim to learn a policy for solving one task, rather than a goal-conditioned policy.

3. Example-Based Control via Recursive Classification

In contrast to standard RL, which uses reward functions, we aim to learn a policy that reaches states that are likely to solve the task (see Fig. 1). After formally defining this problem, we introduce our method, which will be based on recursive classification. This section concludes with analysis of our method

3.1. Problem Statement

We start by formally describing the problem of learning from *examples* of success, which we will call *example-based control*. This problem is defined by a controlled Markov process (i.e., an MDP without a reward function) with dynamics $p(s_{t+1} | s_t, \mathbf{a}_t)$ and an initial state distribution $p_1(s_1)$, where $s_t \in \mathcal{S}$ and \mathbf{a}_t denote the time-indexed states and actions. The agent is given a set of *success examples*, $\mathcal{S}^* = \{s^*\} \subseteq \mathcal{S}$. The binary random variable $e_t \in \{0, 1\}$ indicates whether the task is solved at time t , and $p(e_t | s_t)$ denotes the probability that the current state s_t solves the task. Given a policy $\pi_\phi(\mathbf{a}_t | s_t)$, the (discounted) probability of solving the task at a *future* step is

$$p^\pi(e_{t+} | s_t, \mathbf{a}_t) \triangleq \mathbb{E}_{p^\pi(s_{t+} | s_t, \mathbf{a}_t)} [p(e_{t+} | s_{t+})], \quad (1)$$

where the (discounted) distribution over future states is

$$p^\pi(s_{t+} | s_t, \mathbf{a}_t) \triangleq (1 - \gamma) \sum_{\Delta=0}^{\infty} p^\pi(s_{t+\Delta} = s_{t+} | s_t, \mathbf{a}_t).$$

The variable $s_{t+\Delta}$ denotes a state Δ steps in the future. The example-based control problem is to maximize the likelihood that the task is solved in the (discounted) future:

Definition 1 (Example-based control). *Given a controlled Markov process and distribution over success examples*

$p(s_t | e_t = 1)$, the example-based control problem is to find the policy that optimizes the likelihood of solving the task:

$$\arg \max_{\pi} p^\pi(e_{t+} = 1) = \mathbb{E}_{p_1(s_1)} [p^\pi(e_{t+} = 1 | s_1, a_1)].$$

This objective is equivalent to the standard RL objective with the reward function $r(s_t, \mathbf{a}_t) = p(e_t = 1 | s_t)$. However, we do not assume that we know the probabilities $p(e_t | s_t)$, so we cannot directly apply an off-the-shelf RL algorithm to this task. Instead, we assume that we have samples of successful states, $s^* \sim p_U(s_t | e_t = 1)$. Example-based control is not the same as imitation learning or goal-conditioned RL: imitation learning methods require full expert demonstrations and goal-conditioned RL methods would attempt to visit one single expert state.

Since interacting with the environment to collect experience is expensive in many settings, we define an *off-policy* version of the problem above, where the agent must learn from environment interactions collected from other policies. We call this problem setting *off-policy example-based control*, and use $p(s_t, \mathbf{a}_t, s_{t+1})$ to denote the distribution of off-policy transitions. In this setting, the agent learns from two distinct datasets: off-policy transitions, $\{(s_t, \mathbf{a}_t, s_{t+1}) \sim p(s_t, \mathbf{a}_t, s_{t+1})\}$, which contain information about the environment dynamics; and success examples, $\mathcal{S}^* = \{s^* \sim p(s_t | e_t = 1)\}$, which specify the task that the agent should attempt to solve. Our analysis will assume that these two datasets are fixed. This paper will propose an algorithm for off-policy example-based control.

An assumption on success examples. The probability that each state solves the task, $p(e_t = 1 | s_t)$ cannot be uniquely determined from success examples and transitions alone. For example, some states might only rarely solve the task, but that state might still be included as a success example. This ambiguity is apparent if we try to express the probability that a state solves the task using Bayes' Rule:

$$p(e_t = 1 | s_t) = \frac{p_U(s_t | e_t = 1)}{p_U(s_t)} p_U(e_t = 1), \quad (2)$$

where $p_U(s_t)$ reflects how often the user visited state s_t , regardless of whether that state solved the task. The user may be quite bad at solving the task themselves.

Any method that learns from success examples must make an additional assumption on $p_U(s_t)$ to make the example-based control problem well defined. We will discuss two choices of assumptions, both of which will allow us to determine how to select $p(e_t = 1 | s_t)$ for use in policy search. The **first choice** is to assume that the user visited states with the same frequency that they occur in the dataset of transitions. Formally, we can express this assumption as:

$$p_U(s_t) = \iint p(s_t, \mathbf{a}_t, s_{t+1}) d\mathbf{a}_t ds_{t+1}. \quad (3)$$

Intuitively, this assumption implies that the user has the same capabilities as the agent. Prior work makes this same assumption (Fu et al., 2018b; Singh et al., 2019; Nasiriany, 2020), though it is not explicitly stated. We include a more detailed discussion of this point in Appendix D. Experimentally, we find that our method succeeds even in cases where this assumption is violated.

However, assuming that the user visits the same distribution of states that appears in the dataset of transitions may not be reasonable in many cases. For example, a human user providing an example of a desired outcome for a robot might obtain this example in some other manner (e.g., buying a desired product to show it to the robot so the robot can learn to build this product itself). The **second choice** is to make as few assumptions on $p_U(\mathbf{s}_t)$ as possible, which leads to a *worst-case* formulation. In this formulation, we optimize the policy to be robust to *any* choice of $p_U(\mathbf{s}_t)$. Surprisingly, this setting admits a tractable solution under some assumptions, as we discuss in Sec. 4.2.

3.2. Predicting Future Success by Recursive Classification

We now describe our method for example-based control. We start with the more standard **first choice** for the assumption on $p_U(\mathbf{s}_t)$ (Eq. 3); we discuss the second choice in Sec. 4.2.

Defining the future success classifier. The main idea of our approach is to estimate the probability in Eq. 1 indirectly via a future success classifier. This classifier, $C_\theta^\pi(\mathbf{s}_t, \mathbf{a}_t)$, discriminates between “positive” state-action pairs sampled from the conditional distribution $p^\pi(\mathbf{s}_t, \mathbf{a}_t | \mathbf{e}_{t+} = 1)$ and “negatives” sampled from a marginal distribution $p(\mathbf{s}_t, \mathbf{a}_t)$. Intuitively, this classifier is solving a positive-unlabeled classification task (Elkan & Noto, 2008), where “positives” correspond to transitions that lead to the task being solved in the future. We will use different class-specific weights, using a weight of $p(\mathbf{e}_{t+} = 1)$ for the “positives” and a weight of 1 for the “negatives.” Then, if this classifier is trained perfectly, the Bayes-optimal solution is

$$C_\theta^\pi(\mathbf{s}_t, \mathbf{a}_t) = \frac{p^\pi(\mathbf{s}_t, \mathbf{a}_t | \mathbf{e}_{t+} = 1)p(\mathbf{e}_{t+} = 1)}{p^\pi(\mathbf{s}_t, \mathbf{a}_t | \mathbf{e}_{t+} = 1)p(\mathbf{e}_{t+} = 1) + p(\mathbf{s}_t, \mathbf{a}_t)} \quad (4)$$

The motivation for using these class-specific weights is so that the classifier’s predicted probability ratio tells us the probability of solving the task in the future:

$$\frac{C_\theta^\pi(\mathbf{s}_t, \mathbf{a}_t)}{1 - C_\theta^\pi(\mathbf{s}_t, \mathbf{a}_t)} = p^\pi(\mathbf{e}_{t+} = 1 | \mathbf{s}_t, \mathbf{a}_t). \quad (5)$$

Importantly, the resulting method will not actually require estimating the weight $p(\mathbf{e}_{t+} = 1)$.

Learning the future success classifier. We will represent the classifier C_θ^π as a neural network with parameters θ . We

would like to optimize these parameters using maximum likelihood estimation:

$$\mathcal{L}^\pi(\theta) \triangleq p(\mathbf{e}_{t+} = 1) \mathbb{E}_{p(\mathbf{s}_t, \mathbf{a}_t | \mathbf{e}_{t+} = 1)} [\log C_\theta^\pi(\mathbf{s}_t, \mathbf{a}_t)] + \mathbb{E}_{p(\mathbf{s}_t, \mathbf{a}_t)} [\log(1 - C_\theta^\pi(\mathbf{s}_t, \mathbf{a}_t))]. \quad (6)$$

While we can estimate the second expectation using Monte Carlo samples $(\mathbf{s}_t, \mathbf{a}_t) \sim p(\mathbf{s}_t, \mathbf{a}_t)$, we cannot directly estimate the first expectation because we cannot sample from $(\mathbf{s}_t, \mathbf{a}_t) \sim p(\mathbf{s}_t, \mathbf{a}_t | \mathbf{e}_{t+} = 1)$. We will address this challenge by deriving a method for training the classifier that resembles the temporal difference update used in value-based RL algorithms, such as Q-learning. We will derive our method from Eq. 6 using three steps. The **first step** is to factor the first expectation in Eq. 6

$$p(\mathbf{s}_t, \mathbf{a}_t | \mathbf{e}_{t+} = 1)p(\mathbf{e}_{t+} = 1) = p^\pi(\mathbf{e}_{t+} = 1 | \mathbf{s}_t, \mathbf{a}_t)p(\mathbf{s}_t, \mathbf{a}_t).$$

The **second step** is to observe that the term $p^\pi(\mathbf{e}_{t+} = 1 | \mathbf{s}_t, \mathbf{a}_t)$ satisfies the following recursive identity:

$$p^\pi(\mathbf{e}_{t+} = 1 | \mathbf{s}_t, \mathbf{a}_t) = (1 - \gamma)p(\mathbf{e}_{t+} = 1 | \mathbf{s}_t) + \gamma \mathbb{E}_{p(\mathbf{s}_{t+1} | \mathbf{s}_t, \mathbf{a}_t), \pi_\phi(\mathbf{a}_{t+1} | \mathbf{s}_{t+1})} [p^\pi(\mathbf{e}_{t+} = 1 | \mathbf{s}_{t+1}, \mathbf{a}_{t+1})]. \quad (7)$$

The **third step** is to estimate expectations w.r.t. the first term in Eq. 7 using samples $\mathbf{s}^* \sim p(\mathbf{s}_t | \mathbf{e}_t = 1)$ together with the assumption in Eq. 3. Without loss of generality, we can assume $p_U(\mathbf{e}_{t+} = 1) = 1$, as any other choice simply scales $p^\pi(\mathbf{e}_{t+} = 1 | \mathbf{s}_t, \mathbf{a}_t)$ by a constant and does not affect the resulting policy. The expression $p^\pi(\mathbf{e}_{t+} = 1 | \mathbf{s}_{t+1}, \mathbf{a}_{t+1})$ in Eq. 7 can be estimated using the classifier’s predictions at the next state together with Eq. 5. Substituting these three steps in Eq. 6 we arrive at our final objective:

$$\mathcal{L}^\pi(\theta) = (1 - \gamma) \mathbb{E}_{p_U(\mathbf{s}_t | \mathbf{e}_t = 1), p(\mathbf{a}_t | \mathbf{s}_t)} [\underbrace{\log C_\theta^\pi(\mathbf{s}_t, \mathbf{a}_t)}_{(a)}] + \mathbb{E}_{p(\mathbf{s}_t, \mathbf{a}_t, \mathbf{s}_{t+1})} [\underbrace{\gamma w \log C_\theta^\pi(\mathbf{s}_t, \mathbf{a}_t)}_{(b)} + \underbrace{\log(1 - C_\theta^\pi(\mathbf{s}_t, \mathbf{a}_t))}_{(c)}], \quad (8)$$

where

$$w = \mathbb{E}_{p(\mathbf{a}_{t+1} | \mathbf{s}_{t+1})} \left[\frac{C_\theta^\pi(\mathbf{s}_{t+1}, \mathbf{a}_{t+1})}{1 - C_\theta^\pi(\mathbf{s}_{t+1}, \mathbf{a}_{t+1})} \right] \quad (9)$$

is the classifier’s prediction (ratio) at the next time step. This equation has an intuitive interpretation. The first term **(a)** trains the classifier to predict 1 for the success examples themselves, and the third term **(c)** trains the classifier to predict 0 for random transitions. The important term is the second term **(b)**, which is analogous to the “bootstrapping” term in temporal difference learning (Sutton, 1988). For term **(b)**, the classifier is trained to predict that the probability of future success depends on the probability of success at the *next* time step, as inferred using the classifier’s

converges in the tabular setting, an immediate consequence of Lemma 4.2 is that tabular RCE also converges:

Corollary 4.2.1. *RCE converges in the tabular setting.*

So far we have analyzed the training process for the classifier for a fixed policy. We conclude this section by showing that optimizing the policy w.r.t. the classifier improves the policy’s performance.

Lemma 4.3. *Let policy $\pi(a | s)$ be given, let \mathcal{S}^* denote the set of success examples, and let $C^\pi(\mathbf{s}_t, \mathbf{a}_t)$ denote the corresponding Bayes-optimal classifier. We construct an improved policy by acting greedily w.r.t. C^π : $\pi'(a_t | \mathbf{s}_t) = \mathbb{1}(\mathbf{a} = \arg \max_a C^\pi(\mathbf{s}_t, \mathbf{a}))$. Then the new policy is at least as good as the old policy at solving the task:*

$$p^{\pi'}(\mathbf{e}_{t+} = 1) \geq p^\pi(\mathbf{e}_{t+} = 1).$$

4.2. Robust Example-based Control

In this section, we derive a principled solution for the case where $p_U(\mathbf{s}_t)$ is not known, which will correspond to modifying the objective function for example-based control. However, we will argue that, in some conditions, the method proposed in Sec. 3.2 is *already* robust to unknown $p_U(\mathbf{s}_t)$, if that method is used with online data collection. The goal of this discussion is to provide a theoretical relationship between our method and a robust version of example-based control that makes fewer assumptions about $p_U(\mathbf{s}_t)$. This discussion will also clarify how changing assumptions on the user’s capabilities can change the optimal policy.

When introducing example-based control in Sec. 3.1, we emphasized that we *must* make an assumption to make the example-based control problem well defined. The exact probability that a success example solves the task depends on how easy it was for the user to visit that state, which the agent does not know. Therefore, there are many valid hypotheses for how likely each state is to solve the task. We can express the set of valid hypotheses using Bayes’ Rule:

$$\mathcal{P}_{\mathbf{e}_t | \mathbf{s}_t} \triangleq \left\{ \hat{p}(\mathbf{e}_t = 1 | \mathbf{s}_t) = \frac{p_U(\mathbf{s}_t | \mathbf{e}_t = 1)p(\mathbf{e}_t = 1)}{p_U(\mathbf{s}_t)} \right\}.$$

Previously (Sec. 3.2), we resolved this ambiguity by assuming that $p_U(\mathbf{s}_t)$ was equal to the distribution over states in our replay buffer. However, this modeling assumption is violated in many common settings, such as when the user is subject to different dynamics constraints than the agent. For example, a human user collecting success examples for a cleaning task might usually put away objects on a shelf at eye-level, whereas transitions collected by a robot might be biased towards interacting with the ground-level shelves. Under our previous assumption, the robot would assume that putting objects away on higher shelves is more satisfactory than putting them away on lower shelves, even though doing so might be much more challenging for the robot.

In the absence of any prior knowledge about $p_U(\mathbf{s}_t)$ (e.g., knowledge about the user’s capabilities), we can instead optimize for solving the task assuming the *worst* possible choice of $p_U(\mathbf{s}_t)$. This approach will make the agent robust to imperfect knowledge of the user’s abilities and to mislabeled success examples. Formally, we define this *robust example-based control* problem as follows:

$$\begin{aligned} \max_{\pi} \min_{\hat{p}(\mathbf{e}_t | \mathbf{s}_t) \in \mathcal{P}_{\mathbf{e}_t | \mathbf{s}_t}} \mathbb{E}_{p^\pi(\mathbf{s}_{t+})} [\hat{p}(\mathbf{e}_{t+} = 1 | \mathbf{s}_{t+})] \quad (13) \\ = \max_{\pi} \min_{p_U(\mathbf{s}_t)} \mathbb{E}_{p^\pi(\mathbf{s}_{t+})} \left[\frac{p_U(\mathbf{s}_t | \mathbf{e}_t = 1)}{p_U(\mathbf{s}_t)} p(\mathbf{e}_t = 1) \right]. \end{aligned}$$

As shown on the second line, this objective is equivalent to having the adversary assign a weight of $1/p_U(\mathbf{s}_t)$ to each success example. The optimal adversary will assign lower weights to success examples that the policy frequently visits and higher weights to less-visited success examples. Intuitively, the optimal policy should try to reach many of the success examples, not just the ones that are easiest to reach. Thus, such a policy will continue to succeed even if certain success examples are removed, or are later discovered to have been mislabeled. Surprisingly, solving this two-player game corresponds to minimizing an f -divergence:

Lemma 4.4. *Robust example-based control (Eq. 13) is equivalent to minimizing the squared Hellinger distance between policy’s discounted state occupancy measure and the **conditional** distribution $p(\mathbf{s}_t | \mathbf{e}_t = 1)$:*

$$\min_{\hat{p}(\mathbf{e}_t | \mathbf{s}_t) \in \mathcal{P}_{\mathbf{e}_t | \mathbf{s}_t}} p^{\pi, \hat{p}}(\mathbf{e}_{t+}) = 1 - \frac{1}{2} H^2[p(\mathbf{s}_t | \mathbf{e}_t = 1), p^\pi(\mathbf{s}_{t+} = \mathbf{s}_t)],$$

where $H^2[p, q]$ is the squared Hellinger distance:

$$H^2[p(x), q(x)] = \int (\sqrt{p(x)} - \sqrt{q(x)})^2 dx.$$

Thus, maximizing the robust example-based control objective is equivalent to minimizing this Hellinger distance.

The main idea of the proof (found in Appendix C) is to compute the worst-case distribution $p_U(\mathbf{s}_t)$ using the calculus of variations. Preliminary experiments (Fig. 5 in Appendix C) found that a version of RCE with online data collection finds policies that perform well on the robust example-based control objective (Eq. 13). In fact, under strong assumptions we can show that the solution of robust example-based control is a fixed point of *iterated* RCE (see Appendix C.2.). Therefore, in our experiments, we use RCE with online data collection.

5. Experiments

Our experiments study how effectively RCE solves example-based control tasks, especially in comparison to prior methods that learn an explicit reward function. Both RCE and

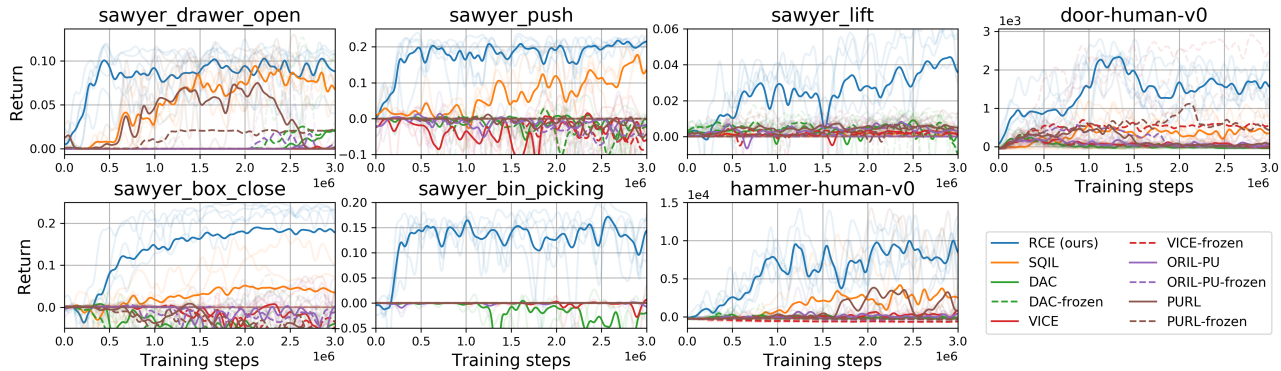


Figure 2. **Recursive Classification of Examples for learning manipulation tasks:** We apply RCE to a range of manipulation tasks, each accompanied with a dataset of success examples. For example, on the `sawyer_lift` task, we provide success examples where the object has been lifted above the table. We use the cumulative task return (\uparrow is better) solely for evaluation. We observe that our method (blue line) outperforms prior methods across all tasks.



Figure 3. **Manipulation Environments**

the prior methods are provided only with success examples as supervision, and no reward function or expert trajectories are provided during training. Our experiments with image observations study whether RCE can solve tasks in new environments that are different from those where the success examples were collected. We include videos of learned policies online¹ and include implementation details, hyperparameters, ablation experiments, and a list of failed experiments in the Appendix.

We compare RCE against prior methods that infer a reward function from the success examples and then apply an off-the-shelf RL algorithm; some baselines iterate between these two steps. AIRL (Fu et al., 2018a) is a popular adversarial imitation learning method. VICE (Fu et al., 2018b) is the same algorithm as AIRL, but intended to be applied to success examples, rather than full demonstrations. We will label this method as “VICE” in figures, noting that it is the exact same algorithm as AIRL. DAC (Kostrikov et al., 2018) is a more recent, off-policy variant of AIRL. We also compared against two recent methods that learn rewards from *demonstrations*: ORIL (Zolna et al., 2020) and PURL (Xu & Denil, 2019). Following prior work (Konyushkova et al., 2020), we also compare against “frozen” variants of some baselines that first train the parameters of the reward function and then apply RL to that reward function without updating the parameters of the reward function again. Our method differs from these baselines in that we do not learn a reward function from the success examples and then apply RL, but rather learns a policy directly from the success

examples. Lastly, we compare against SQIL (Reddy et al., 2020), an imitation learning method that assigns a reward of +1 to states from demonstrations and 0 to all other states. SQIL does not learn a separate reward function and structurally resembles our method, but is derived from different principles (see Sec. 2.).

5.1. Learning Manipulation Tasks

We evaluate each method on five Sawyer manipulation tasks from Meta-World Yu et al. (2020) and two Adept manipulation tasks from Rajeswaran et al. (2018), shown in Fig. 3. On each task, we provide the agent with 200 successful outcomes to define the task. For example, on the `open_drawer` task, these success examples show an opened drawer. We emphasize that these success examples only reflect the solved task, and are not entire trajectories from an expert policy. This is important in practical use-cases: it is often easier for humans to arrange the workspace into a successful configuration than it is to collect an entire demonstration. See Appendix E.3 for details on how success examples were generated for each task. The tasks we use come with existing user-defined reward functions, which are not provided to any of the methods in our experiments, but are used for evaluation only. The results in Fig. 2 show this return (\uparrow is better) as a way to compare the different methods. The reward functions for the Sawyer tasks contain many additional reward shaping terms, which we remove to more directly evaluate success. Across all tasks, we observe that RCE outperforms prior methods, especially for the more challenging hammering and picking tasks. Most prior methods that tackle similar tasks employ hand-designed reward functions or distance functions, full demonstrations, or carefully-constructed initial state distributions.

¹<https://ben-eysenbach.github.io/rce>

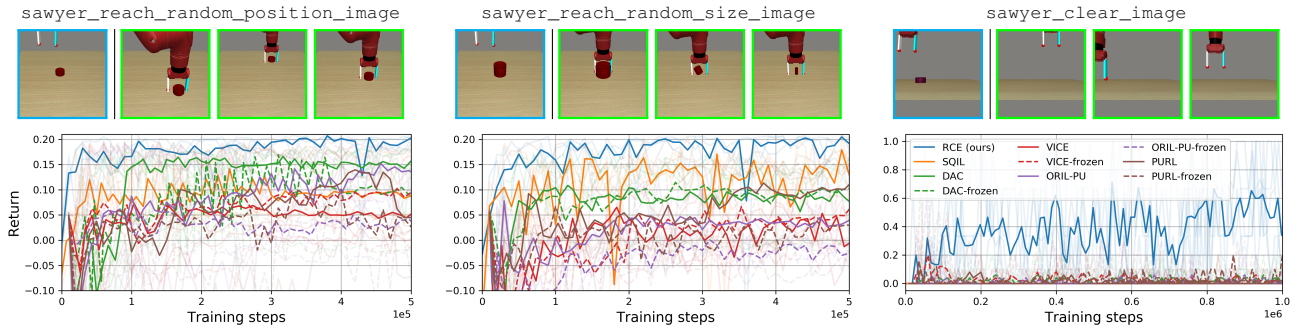


Figure 4. **Example-based control from images:** We evaluate RCE on three manipulation tasks using image-observations. (Top) We show examples of the initial state and success examples for each task. (Bottom) RCE (blue line) outperforms prior methods, especially on the more challenging clearing task. For the random_size task (center), this entails reaching for new objects that have different sizes from any seen in the success examples.

5.2. Example-Based Control from Images

Our second set of experiments study whether RCE can learn image-based tasks and assess the generalization capabilities of our method. To this end, we designed three image-based manipulation tasks. The reach_random_position task entails reaching a red puck, whose position is randomized in each episode. The reach_random_size task entails reaching a red object, but the actual shape of that object varies from one episode to the next. Since the agent cannot change the size of the object and the size is randomized from one episode to the next, it is impossible to reach any of the previously-observed success examples. To solve this task, the agent must learn a notion of “success” that is more general than reaching a fixed goal state. The third task, sawyer_clear_image, entails clearing an object off the table, and is mechanically more challenging than the reaching tasks.

Fig. 4 shows results from these image-based experiments, comparing RCE to the same baselines. We observe that RCE has learned to solve both reaching tasks, reaching for the object regardless of the location and size of the object. This task is mechanically easier than the state-based tasks in Fig. 2, and all the baselines make some progress on this task, but learn more slowly than our method. The good performance of RCE on the reach_random_size task illustrates that RCE can solve tasks in a new environment, where the object size is different from that seen in the success examples. We hypothesize that RCE learns faster than these baselines because it “cuts out the middleman,” learning a value function directly from examples rather than indirectly via a separate success classifier. To support this hypothesis, we note SQIL, which also avoids learning an intermediary classifier, learns faster than other baselines on the second variation. On the more challenging clearing task, only our method makes progress, suggesting that RCE is a more effective algorithm for learning these image-based control tasks. In summary, these results show that RCE

outperforms prior methods at solving example-based control tasks from image observations, and highlights that RCE learns a policy that solves tasks in new environments that look different from any of the success examples.

6. Conclusion

In this paper, we proposed a data-driven approach to control, where examples of success states are used in place of a reward function. We then introduced a method for estimating the probability of reaching a success example in the future and optimizing a policy to maximize this probability of success. Unlike prior imitation learning methods, our approach is “end-to-end” and does not require learning an auxiliary classifier or reward function. Our method is therefore simpler, with fewer hyperparameters and fewer lines of code to debug. Our analysis rests on a new data-driven Bellman equation, where example success states replace the typical reward function term. We use this Bellman equation to prove convergence of our classifier and policy.

Limitations and future work. Empirically, we observed that the classifier’s predictions were not well calibrated but nonetheless produced an effective policy. This issue resembles the miscalibration in Q-functions observed in prior work (Lillicrap et al., 2016; Fujimoto et al., 2018). In future work we aim to develop better off-policy evaluation techniques for example-based control to lift this limitation. On the algorithmic side, we encourage future work on multi-task and language-driven variants of example-based control. We believe that formulating control problems in terms of data, rather than the reward-centric MDP, better captures the essence of many real-world control problems and suggests a new set of attractive learning algorithms.

Acknowledgements. This work is supported by the Fannie and John Hertz Foundation, NSF (DGE1745016, IIS1763562), ONR (N000141812861), and US Army. We thank Ilya Kostrikov for providing the implementation of DAC. We thank Ksenia

Konyushkova, Konrad Zolna, and Justin Fu for discussions about baselines and prior work. We thank Oscar Ramirez for help setting up the image-based experiments, Ryan Julian for feedback on a draft of the paper, and Alex Irpan for help releasing code.

References

- Abbeel, P. and Ng, A. Y. Apprenticeship learning via inverse reinforcement learning. In *Proceedings of the twenty-first international conference on Machine learning*, pp. 1, 2004.
- Barreto, A., Dabney, W., Munos, R., Hunt, J. J., Schaul, T., van Hasselt, H. P., and Silver, D. Successor features for transfer in reinforcement learning. In *Advances in neural information processing systems*, pp. 4055–4065, 2017.
- Calandra, R., Owens, A., Upadhyaya, M., Yuan, W., Lin, J., Adelson, E. H., and Levine, S. The feeling of success: Does touch sensing help predict grasp outcomes? In *Conference on Robot Learning*, pp. 314–323. PMLR, 2017.
- Dayan, P. Improving generalization for temporal difference learning: The successor representation. *Neural Computation*, 5(4): 613–624, 1993.
- Elkan, C. and Noto, K. Learning classifiers from only positive and unlabeled data. In *Proceedings of the 14th ACM SIGKDD international conference on Knowledge discovery and data mining*, pp. 213–220, 2008.
- Eysenbach, B., Salakhutdinov, R., and Levine, S. C-learning: Learning to achieve goals via recursive classification. In *International Conference on Learning Representations*, 2021. URL <https://openreview.net/forum?id=tc5qisoB-C>.
- Fox, R., Pakman, A., and Tishby, N. Taming the noise in reinforcement learning via soft updates. *arXiv preprint arXiv:1512.08562*, 2015.
- Fu, J., Luo, K., and Levine, S. Learning robust rewards with adversarial inverse reinforcement learning. In *International Conference on Learning Representations*, 2018a.
- Fu, J., Singh, A., Ghosh, D., Yang, L., and Levine, S. Variational inverse control with events: A general framework for data-driven reward definition. *Advances in neural information processing systems*, 31:8538–8547, 2018b.
- Fu, J., Kumar, A., Nachum, O., Tucker, G., and Levine, S. D4rl: Datasets for deep data-driven reinforcement learning. *arXiv preprint arXiv:2004.07219*, 2020.
- Fujimoto, S., Hoof, H., and Meger, D. Addressing function approximation error in actor-critic methods. In *International Conference on Machine Learning*, pp. 1587–1596. PMLR, 2018.
- Guadarrama, S., Korattikara, A., Ramirez, O., Castro, P., Holly, E., Fishman, S., Wang, K., Gonina, E., Wu, N., Kokiopoulou, E., Sbaiz, L., Smith, J., Bartók, G., Berent, J., Harris, C., Vanhoucke, V., and Brevedo, E. TF-Agents: A library for reinforcement learning in tensorflow, 2018. URL <https://github.com/tensorflow/agents>. [Online; accessed 25-June-2019].
- Haarnoja, T., Zhou, A., Abbeel, P., and Levine, S. Soft actor-critic: Off-policy maximum entropy deep reinforcement learning with a stochastic actor. In *International Conference on Machine Learning*, pp. 1861–1870. PMLR, 2018.
- Ho, J. and Ermon, S. Generative adversarial imitation learning. In *NIPS*, pp. 4565–4573, 2016.
- Irpan, A., Rao, K., Bousmalis, K., Harris, C., Ibarz, J., and Levine, S. Off-policy evaluation via off-policy classification. In *Advances in Neural Information Processing Systems*, pp. 5437–5448, 2019.
- Jaakkola, T., Jordan, M. I., and Singh, S. P. On the convergence of stochastic iterative dynamic programming algorithms. *Neural computation*, 6(6):1185–1201, 1994.
- Konyushkova, K., Zolna, K., Aytar, Y., Novikov, A., Reed, S., Cabi, S., and de Freitas, N. Semi-supervised reward learning for off-line reinforcement learning. *arXiv preprint arXiv:2012.06899*, 2020.
- Kostrikov, I., Agrawal, K. K., Dwibedi, D., Levine, S., and Tompson, J. Discriminator-actor-critic: Addressing sample inefficiency and reward bias in adversarial imitation learning. In *International Conference on Learning Representations*, 2018.
- Kostrikov, I., Nachum, O., and Tompson, J. Imitation learning via off-policy distribution matching. In *International Conference on Learning Representations*, 2019.
- Kulkarni, T. D., Saeedi, A., Gautam, S., and Gershman, S. J. Deep successor reinforcement learning. *arXiv preprint arXiv:1606.02396*, 2016.
- Lillicrap, T. P., Hunt, J. J., Pritzel, A., Heess, N., Erez, T., Tassa, Y., Silver, D., and Wierstra, D. Continuous control with deep reinforcement learning. In *ICLR (Poster)*, 2016. URL <http://arxiv.org/abs/1509.02971>.
- Lu, Q., Van der Merwe, M., Sundaralingam, B., and Hermans, T. Multi-fingered grasp planning via inference in deep neural networks. *arXiv preprint arXiv:2001.09242*, 2020.
- Nasiriany, S. *DisCo RL: Distribution-Conditioned Reinforcement Learning for General-Purpose Policies*. PhD thesis, 2020.
- Pomerleau, D. A. Alvinn: An autonomous land vehicle in a neural network. In *Advances in neural information processing systems*, pp. 305–313, 1989.
- Rajeswaran, A., Kumar, V., Gupta, A., Vezzani, G., Schulman, J., Todorov, E., and Levine, S. Learning Complex Dexterous Manipulation with Deep Reinforcement Learning and Demonstrations. In *Proceedings of Robotics: Science and Systems (RSS)*, 2018.
- Ratliff, N. D., Bagnell, J. A., and Zinkevich, M. A. Maximum margin planning. In *Proceedings of the 23rd international conference on Machine learning*, pp. 729–736, 2006.
- Reddy, S., Dragan, A. D., and Levine, S. {SQL}: Imitation learning via reinforcement learning with sparse rewards. In *International Conference on Learning Representations*, 2020. URL <https://openreview.net/forum?id=SlxKd24twB>.

- Ross, S., Gordon, G., and Bagnell, D. A reduction of imitation learning and structured prediction to no-regret online learning. In *Proceedings of the fourteenth international conference on artificial intelligence and statistics*, pp. 627–635, 2011.
- Schaul, T., Horgan, D., Gregor, K., and Silver, D. Universal value function approximators. In *International conference on machine learning*, pp. 1312–1320, 2015.
- Singh, A., Yang, L., Finn, C., and Levine, S. End-to-end robotic reinforcement learning without reward engineering. In *Robotics: Science and Systems*, 2019.
- Srinivas, A., Laskin, M., and Abbeel, P. Curl: Contrastive unsupervised representations for reinforcement learning. *CoRR*, abs/2004.04136, 2020. URL <https://arxiv.org/abs/2004.04136>.
- Sutton, R. S. Learning to predict by the methods of temporal differences. *Machine learning*, 3(1):9–44, 1988.
- Sutton, R. S. Td models: Modeling the world at a mixture of time scales. In *Machine Learning Proceedings 1995*, pp. 531–539. Elsevier, 1995.
- Vecerik, M., Sushkov, O., Barker, D., Rothörl, T., Hester, T., and Scholz, J. A practical approach to insertion with variable socket position using deep reinforcement learning. In *2019 International Conference on Robotics and Automation (ICRA)*, pp. 754–760. IEEE, 2019.
- Williams, R. J. and Peng, J. Function optimization using connectionist reinforcement learning algorithms. *Connection Science*, 3(3):241–268, 1991.
- Wulfmeier, M., Ondruska, P., and Posner, I. Maximum entropy deep inverse reinforcement learning. *arXiv preprint arXiv:1507.04888*, 2015.
- Xie, A., Singh, A., Levine, S., and Finn, C. Few-shot goal inference for visuomotor learning and planning. In *Conference on Robot Learning*, pp. 40–52. PMLR, 2018.
- Xu, D. and Denil, M. Positive-unlabeled reward learning. *arXiv preprint arXiv:1911.00459*, 2019.
- Yu, T., Quillen, D., He, Z., Julian, R., Hausman, K., Finn, C., and Levine, S. Meta-world: A benchmark and evaluation for multi-task and meta reinforcement learning. In *Conference on Robot Learning*, pp. 1094–1100. PMLR, 2020.
- Ziebart, B. D., Maas, A. L., Bagnell, J. A., and Dey, A. K. Maximum entropy inverse reinforcement learning. In *Aaai*, volume 8, pp. 1433–1438. Chicago, IL, USA, 2008.
- Zolna, K., Reed, S., Novikov, A., Colmenarej, S. G., Budden, D., Cabi, S., Denil, M., de Freitas, N., and Wang, Z. Task-relevant adversarial imitation learning. *arXiv preprint arXiv:1910.01077*, 2019.
- Zolna, K., Novikov, A., Konyushkova, K., Gulcehre, C., Wang, Z., Aytaç, Y., Denil, M., de Freitas, N., and Reed, S. Offline learning from demonstrations and unlabeled experience. *arXiv preprint arXiv:2011.13885*, 2020.

A. Derivation of Recursive Classification of Examples

In this section we include the full derivation of our method (RCE), based on the ideas introduced in Sec. 3.2. Recall that the objective we would like to optimize (Eq. 6) is

$$\mathcal{L}^\pi(\theta) \triangleq p(\mathbf{e}_{t+} = 1) \mathbb{E}_{p(\mathbf{s}_t, \mathbf{a}_t | \mathbf{e}_{t+}=1)} [\log C_\theta^{(t)}] + \mathbb{E}_{p(\mathbf{s}_t, \mathbf{a}_t)} [\log(1 - C_\theta^{(t)})].$$

We start by substituting the identity from the **first step**, and then combine terms on the second line.

$$\begin{aligned} \mathcal{L}^\pi(\theta) &= \mathbb{E}_{p(\mathbf{s}_t, \mathbf{a}_t)} [p^\pi(\mathbf{e}_{t+} = 1 | \mathbf{s}_t, \mathbf{a}_t) \log C_\theta^{(t)}] + \mathbb{E}_{p(\mathbf{s}_t, \mathbf{a}_t)} [\log(1 - C_\theta^{(t)})] \\ &= \mathbb{E}_{p(\mathbf{s}_t, \mathbf{a}_t)} [p^\pi(\mathbf{e}_{t+} = 1 | \mathbf{s}_t, \mathbf{a}_t) \log C_\theta^{(t)} + \log(1 - C_\theta^{(t)})]. \end{aligned}$$

We then replace $p^\pi(\mathbf{e}_{t+} = 1 | \mathbf{s}_t, \mathbf{a}_t)$ with the identity from the **second step** (Eq. 7), and then break the expectation into two terms.

$$\begin{aligned} \mathcal{L}^\pi(\theta) &= \mathbb{E}_{p(\mathbf{s}_t, \mathbf{a}_t)} \left[\left((1 - \gamma)p(\mathbf{e}_t = 1 | \mathbf{s}_t) + \gamma \mathbb{E}_{\substack{p(\mathbf{s}_{t+1} | \mathbf{s}_t, \mathbf{a}_t), \\ \pi_\phi(\mathbf{a}_{t+1} | \mathbf{s}_{t+1})}} [p^\pi(\mathbf{e}_{t+} = 1 | \mathbf{s}_{t+1}, \mathbf{a}_{t+1})] \right) \log C_\theta^{(t)} + \log(1 - C_\theta^{(t)}) \right] \\ &= (1 - \gamma) \mathbb{E}_{p(\mathbf{s}_t, \mathbf{a}_t)} \left[p(\mathbf{e}_t = 1 | \mathbf{s}_t) \log C_\theta^{(t)} \right] \\ &\quad + \gamma \mathbb{E}_{p(\mathbf{s}_t, \mathbf{a}_t)} \left[\mathbb{E}_{\substack{p(\mathbf{s}_{t+1} | \mathbf{s}_t, \mathbf{a}_t), \\ \pi_\phi(\mathbf{a}_{t+1} | \mathbf{s}_{t+1})}} [p^\pi(\mathbf{e}_{t+} = 1 | \mathbf{s}_{t+1}, \mathbf{a}_{t+1})] \log C_\theta^{(t)} + \log(1 - C_\theta^{(t)}) \right]. \end{aligned} \quad (14)$$

Next, we use Bayes' Rule from the **third step** to express the first expectation in terms of samples of success example, $\mathbf{s}^* \sim p(\mathbf{s}_t | \mathbf{e}_t = 1)$, and continue by rearranging terms.

$$\begin{aligned} \mathbb{E}_{p(\mathbf{s}_t, \mathbf{a}_t)} \left[p(\mathbf{e}_t = 1 | \mathbf{s}_t) \log C_\theta^{(t)} \right] &= \mathbb{E}_{p(\mathbf{s}_t, \mathbf{a}_t)} \left[\frac{p_U(\mathbf{s}_t | \mathbf{e}_t = 1)}{p(\mathbf{s}_t)} p_U(\mathbf{e}_t = 1) \log C_\theta^{(t)} \right] \\ &= p_U(\mathbf{e}_t = 1) \mathbb{E}_{\substack{p(\mathbf{s}_t), \\ p(\mathbf{a}_t | \mathbf{s}_t)}} \left[\frac{p_U(\mathbf{s}_t | \mathbf{e}_t = 1)}{p(\mathbf{s}_t)} \log C_\theta^{(t)} \right] \\ &= p_U(\mathbf{e}_t = 1) \mathbb{E}_{\substack{p_U(\mathbf{s}_t | \mathbf{e}_t = 1), \\ p(\mathbf{a}_t | \mathbf{s}_t)}} \left[\log C_\theta^{(t)} \right]. \end{aligned}$$

Note that actions are sampled from $p(\mathbf{a}_t | \mathbf{s}_t) = p(\mathbf{s}_t, \mathbf{a}_t) / p(\mathbf{s}_t)$, the average policy used to collect the dataset of transitions. Finally, we substitute this expression back into Eq. 14, and use Eq. 5 to estimate the probability of future success at time $t + 1$.

$$\begin{aligned} \mathcal{L}^\pi(\theta) &= (1 - \gamma) p_U(\mathbf{e}_t = 1) \mathbb{E}_{\substack{p_U(\mathbf{s}_t | \mathbf{e}_t = 1), \\ p(\mathbf{a}_t | \mathbf{s}_t)}} \left[\log C_\theta^{(t)} \right] \\ &\quad + \gamma \mathbb{E}_{p(\mathbf{s}_t, \mathbf{a}_t)} \left[\mathbb{E}_{\substack{p(\mathbf{s}_{t+1} | \mathbf{s}_t, \mathbf{a}_t), \\ \pi_\phi(\mathbf{a}_{t+1} | \mathbf{s}_{t+1})}} \left[\frac{C_\theta^{(t+1)}}{1 - C_\theta^{(t+1)}} \right] \log C_\theta^{(t)} + \log(1 - C_\theta^{(t)}) \right]. \end{aligned}$$

Thus, we have arrived at our final objective (Eq. 8).

B. Proofs

In this section we include proofs of the theoretical results in the main text.

Proof of Lemma 4.1

Proof. To start, we recall that Eq. 5 says that the Bayes-optimal classifier satisfies

$$\frac{C^\pi(\mathbf{s}_t, \mathbf{a}_t)}{1 - C^\pi(\mathbf{s}_t, \mathbf{a}_t)} = p^\pi(\mathbf{e}_{t+} = 1 | \mathbf{s}_t, \mathbf{a}_t).$$

Substituting this identity into both the LHS and RHS of the recursive definition of $p^\pi(\mathbf{e}_{t+} = 1 \mid \mathbf{s}_t, \mathbf{a}_t)$ (Eq. 7), we obtain the desired result:

$$\frac{C^\pi(\mathbf{s}_t, \mathbf{a}_t)}{1 - C^\pi(\mathbf{s}_t, \mathbf{a}_t)} = (1 - \gamma)p^\pi(\mathbf{e}_t = 1 \mid \mathbf{s}_t) + \gamma \mathbb{E}_{\substack{p(\mathbf{s}_{t+1} \mid \mathbf{s}_t, \mathbf{a}_t) \\ \pi(\mathbf{a}_{t+1} \mid \mathbf{s}_{t+1})}} \left[\frac{C^\pi(\mathbf{s}_{t+1}, \mathbf{a}_{t+1})}{1 - C^\pi(\mathbf{s}_{t+1}, \mathbf{a}_{t+1})} \right].$$

□

Proof of Lemma 4.2.1

Proof. We will show that RCE is equivalent to using value iteration using the Bellman equation above, where $(1 - \gamma)p(\mathbf{e}_{t+1} = 1 \mid \mathbf{s}_t, \mathbf{a}_t)$ takes the role of the reward function. For given transition $(\mathbf{s}_t, \mathbf{a}_t, \mathbf{s}_{t+1})$, the corresponding TD target y is the expected value of three terms (Eq. 8): with weight $(1 - \gamma)p(\mathbf{e}_t = 1 \mid \mathbf{s}_t)$ it is assigned $y = 1$; with weight $\gamma\mathbb{E}[w]$ it is assigned label $y = 1$; and with weight 1 it is assigned label $y = 0$. Thus, the expected value of the TD target y can be written as follows:

$$\mathbb{E}[y \mid \mathbf{s}_t, \mathbf{a}_t, \mathbf{s}_{t+1}] = \frac{(1 - \gamma)p(\mathbf{e}_t = 1 \mid \mathbf{s}_t) \cdot 1 + \gamma\mathbb{E}[w] \cdot 1 + 1 \cdot 0}{(1 - \gamma)p(\mathbf{e}_t = 1 \mid \mathbf{s}_t) + \gamma\mathbb{E}[w] + 1}.$$

Thus, the assignment equation can be written as follows:

$$C^\pi(\mathbf{s}_t, \mathbf{a}_t) \leftarrow \mathbb{E}[y \mid \mathbf{s}_t, \mathbf{a}_t, \mathbf{s}_{t+1}] = \frac{(1 - \gamma)p(\mathbf{e}_t = 1 \mid \mathbf{s}_t) + \gamma\mathbb{E}[w]}{(1 - \gamma)p(\mathbf{e}_t = 1 \mid \mathbf{s}_t) + \gamma\mathbb{E}[w] + 1}. \quad (15)$$

While this gives us an assignment equation for C , our Bellman equation is expressed in terms of the *ratio* $C/(1 - C)$. Noting that the function $C/(1 - C)$ is strictly monotone increasing, we can write the same assignment equation for the ratio as follows:

$$\frac{C^\pi(\mathbf{s}_t, \mathbf{a}_t)}{1 - C^\pi(\mathbf{s}_t, \mathbf{a}_t)} \leftarrow \frac{\mathbb{E}[y \mid \mathbf{s}_t, \mathbf{a}_t, \mathbf{s}_{t+1}]}{1 - \mathbb{E}[y \mid \mathbf{s}_t, \mathbf{a}_t, \mathbf{s}_{t+1}]} = (1 - \gamma)p(\mathbf{e}_t = 1 \mid \mathbf{s}_t) + \gamma\mathbb{E}[w].$$

Recalling that $w = \frac{C(\mathbf{s}_{t+1}, \mathbf{a}_{t+1})}{1 - C(\mathbf{s}_{t+1}, \mathbf{a}_{t+1})}$, we conclude that our temporal difference method is equivalent to doing value iteration using the Bellman equation in Eq. 12. □

Proof of Corollary 4.2.1

Proof. Lemma 4.2 showed that the update rule for our method is equivalent to value iteration. Value iteration is known to converge in the tabular setting (Jaakkola et al., 1994, Theorem 1), so our method also converges. □

Proof of Lemma 4.3 The proof of Lemma 4.3 is nearly identical to the standard policy improvement proof for Q-learning.

Proof.

$$\begin{aligned} p^\pi(\mathbf{e}_{t+} = 1) &= \mathbb{E}_{p_0(s), \pi(a_0|s_0)} [p^\pi(\mathbf{e}_{t+} = 1 \mid s_0, a_0)] \\ &\leq \mathbb{E}_{p_0(s), \pi'(a_0|s_0)} [p^\pi(\mathbf{e}_{t+} = 1 \mid s_0, a_0)] \\ &= \mathbb{E}_{p_0(s), \pi'(a_0|s_0)} [(1 - \gamma)p(e_0 = 1 \mid s_0, a_0) + \gamma\mathbb{E}_{p(s_1|s_0, a_0), \pi(a_1|s_1)} [p^\pi(\mathbf{e}_{t+} = 1 \mid s_1, a_1)]] \\ &\leq \mathbb{E}_{p_0(s), \pi'(a_0|s_0)} [(1 - \gamma)p(e_0 = 1 \mid s_0, a_0) + \gamma\mathbb{E}_{p(s_1|s_0, a_0), \pi'(a_1|s_1)} [p^\pi(\mathbf{e}_{t+} = 1 \mid s_1, a_1)]] \\ &= \mathbb{E}_{\substack{p_0(s), \pi'(a_0|s_0) \\ p(s_1|s_0, a_0), \pi'(a_1|s_1)}} [(1 - \gamma)p(e_0 = 1 \mid s_0, a_0) + \gamma p(e_1 = 1 \mid s_1, a_1) \\ &\quad + \gamma^2 \mathbb{E}_{p(s_2|s_1, a_1), \pi(a_2|s_2)} [p^\pi(\mathbf{e}_{t+} = 1 \mid s_2, a_2)]] \\ &\dots \\ &\leq p^{\pi'}(\mathbf{e}_{t+} = 1) \end{aligned}$$

□

C. Robust Example-Based Control

Our strategy for analyzing robust example-based control will be to first compute an analytic solution to the inner minimization problem. Plugging in the optimal adversary, we will find that we weight the success examples inversely based on how often our policy utilizes each of the potential solution strategies.

C.1. Proof of Lemma 4.4

Proof. First, we solve the inner minimization problem. Note that the adversary's choice of an example probability function $\hat{p}(\mathbf{e}_t | \mathbf{s}_t)$ is equivalent to a choice of a marginal distribution, $p_U(\mathbf{s}_t)$. We can write the inner minimization problem as follows:

$$\min_{p_U(\mathbf{s}_t)} \int p^\pi(\mathbf{s}_{t+} = \mathbf{s}_t) \frac{p_U(\mathbf{s}_t | \mathbf{e}_t = 1) p(\mathbf{e}_t = 1)}{p_U(\mathbf{s}_t)} d\mathbf{s}_t \quad (16)$$

As before, we can ignore the constant $p(\mathbf{e}_t = 1)$. We solve this optimization problem, subject to the constraint that $\int p_U(\mathbf{s}_t) d\mathbf{s}_t = 1$, using calculus of variations. The corresponding Lagrangian is

$$\mathcal{L}(p_U, \lambda) = \int \frac{p^\pi(\mathbf{s}_{t+} = \mathbf{s}_t) p_U(\mathbf{s}_t | \mathbf{e}_t = 1)}{p_U(\mathbf{s}_t)} d\mathbf{s}_t + \lambda \left(\int p_U(\mathbf{s}_t) d\mathbf{s}_t - 1 \right). \quad (17)$$

Setting the derivative $\frac{d\mathcal{L}}{dp_U(\mathbf{s}_t)} = 0$, we get

$$-\frac{p^\pi(\mathbf{s}_{t+} = \mathbf{s}_t) p_U(\mathbf{s}_t | \mathbf{e}_t = 1)}{p_U^2(\mathbf{s}_t)} + \lambda = 1 \implies p_U(\mathbf{s}_t) = \frac{\sqrt{p^\pi(\mathbf{s}_{t+} = \mathbf{s}_t) p_U(\mathbf{s}_t | \mathbf{e}_t = 1)}}{\int \sqrt{p^\pi(\mathbf{s}_{t+} = \mathbf{s}_t') p_U(\mathbf{s}_t' | \mathbf{e}_t = 1)} d\mathbf{s}_t'}. \quad (18)$$

Note that $\frac{d^2\mathcal{L}}{dp_U(\mathbf{s}_t)^2} > 0$, so this stationary point is a minimum. We can therefore write the worst-case probability function as

$$\hat{p}(\mathbf{e}_t = 1 | \mathbf{s}_t) = \frac{p_U(\mathbf{s}_t | \mathbf{e}_t = 1)}{p_U(\mathbf{s}_t)} p(\mathbf{e}_t = 1) \quad (19)$$

$$= \sqrt{\frac{p_U(\mathbf{s}_t | \mathbf{e}_t = 1)}{p^\pi(\mathbf{s}_{t+} = \mathbf{s}_t)}} \int \sqrt{p^\pi(\mathbf{s}_{t+} = \mathbf{s}_t') p_U(\mathbf{s}_t' | \mathbf{e}_t = 1)} d\mathbf{s}_t' p(\mathbf{e}_t = 1). \quad (20)$$

Intuitively, this says that the worst-case probability function is one where successful states $\mathbf{s}_t \sim p_U(\mathbf{s}_t | \mathbf{e}_t = 1)$ are downweighted if the current policy visits those states more frequently (i.e., if $p^\pi(\mathbf{s}_{t+} = \mathbf{s}_t)$ is large). Substituting this worst-case example probability into Eq. 13, we can write the adversarial objective as follows:

$$\max_{\pi} \int p^\pi(\mathbf{s}_{t+} = \mathbf{s}_t) \sqrt{\frac{p_U(\mathbf{s}_t | \mathbf{e}_t = 1)}{p^\pi(\mathbf{s}_{t+} = \mathbf{s}_t)}} d\mathbf{s}_t \int \sqrt{p^\pi(\mathbf{s}_{t+} = \mathbf{s}_t') p_U(\mathbf{s}_t' | \mathbf{e}_t = 1)} d\mathbf{s}_t' p(\mathbf{e}_t = 1) \quad (21)$$

$$= \left(\int \sqrt{p^\pi(\mathbf{s}_{t+} = \mathbf{s}_t) p_U(\mathbf{s}_t | \mathbf{e}_t = 1)} d\mathbf{s}_t \right)^2 p(\mathbf{e}_t = 1) \quad (22)$$

Since $p(\mathbf{e}_t = 1)$ is assumed to be a constant and $(\cdot)^2$ is a monotone increasing function (for non-negative arguments), we can express this same optimization problem as follows:

$$\max_{\pi} \int \sqrt{p^\pi(\mathbf{s}_{t+} = \mathbf{s}_t) p_U(\mathbf{s}_t | \mathbf{e}_t = 1)} d\mathbf{s}_t. \quad (23)$$

Using a bit of algebra, we can show that this objective is a (scaled and shifted) squared Hellinger distance:

$$\int \sqrt{p^\pi(\mathbf{s}_{t+} = \mathbf{s}_t)} p_U(\mathbf{s}_t | \mathbf{e}_t = 1) d\mathbf{s}_t \quad (24)$$

$$= 1 - \frac{1}{2} \int \left(\sqrt{p^\pi(\mathbf{s}_{t+} = \mathbf{s}_t)} - \sqrt{p_U(\mathbf{s}_t | \mathbf{e}_t = 1)} \right)^2 d\mathbf{s}_t \quad (25)$$

$$= 1 - \frac{1}{2} \int \left(\sqrt{p_U(\mathbf{s}_t | \mathbf{e}_t = 1)} \left(\sqrt{\frac{p^\pi(\mathbf{s}_{t+} = \mathbf{s}_t)}{p_U(\mathbf{s}_t | \mathbf{e}_t = 1)}} - 1 \right) \right)^2 d\mathbf{s}_t \quad (26)$$

$$= 1 - \frac{1}{2} \mathbb{E}_{p_U(\mathbf{s}_t | \mathbf{e}_t = 1)} \left[\left(1 - \sqrt{\frac{p^\pi(\mathbf{s}_{t+} = \mathbf{s}_t)}{p_U(\mathbf{s}_t | \mathbf{e}_t = 1)}} \right)^2 \right] \quad (27)$$

$$= 1 - \frac{1}{2} H^2(p_U(\mathbf{s}_t | \mathbf{e}_t = 1), p^\pi(\mathbf{s}_{t+} = \mathbf{s}_t)). \quad (28)$$

□

C.2. Robust Example-Based Control and Iterated RCE

As noted in Sec. 4.2, we found empirically that the policy found by RCE with online data collection was similar to the optimal policy for the robust example-based control objective. We visualize that experiment in Fig. 5. In this 2D navigation task there are two sets of success examples (orange circles). When we apply RCE to this task using a uniform distribution of transitions, the agent navigates directly towards the closer success examples. However, when we run RCE in an iterative fashion, periodically collecting data from the current policy, the final policy visits both sets of success examples. This behavior is similar to what we would expect from the optimal policy to robust example-based control. We hypothesize that this happens because our implementation of RCE periodically collects new data using the current policy, violating the assumption that the dataset of transitions $p(\mathbf{s}_t, \mathbf{a}_t, \mathbf{s}_{t+1})$ is fixed. When the policy frequently visits one success example, that state will be included many times in the dataset of transitions $p(\mathbf{s}_t, \mathbf{a}_t, \mathbf{s}_{t+1})$ at the next iteration, so the classifier’s predictions will decrease for that state.

We now show that (under a very strong assumption), the solution to the robust example-based control problem is a fixed point of an iterative version of RCE. The iterated version of RCE is defined by alternating between collecting a dataset of transitions using the current policy and then running RCE (Alg. 1) on those trajectories:

$$\begin{aligned} \pi &\leftarrow \text{RCE}(\mathcal{S}^*, \mathcal{D}) \\ \mathcal{D} &\leftarrow \{\tau \sim \pi\} \end{aligned}$$

Lemma C.1. *Let π be an optimal policy for robust example-based control (Eq. 13). Assume that π visits each success example with probability proportional to how often that state occurs as a success example:*

$$\exists 0 < c \leq 1 \text{ s.t. } p^\pi(\mathbf{s}_{t+} = s) = c \cdot p(\mathbf{s}_t = s | \mathbf{e}_t = 1) \forall s \in \mathcal{S}. \quad (29)$$

Then π is a fixed point for iterated RCE.

Proof. If $p^\pi(\mathbf{s}_{t+}) = p(\mathbf{s}_t | \mathbf{e}_t = 1)$, then Eq. 2 tells us that $p(\mathbf{e}_t = 1 | \mathbf{s}_t)$ is a constant for all states. In this setting, all policies are optimal under our objective (Def. 1), so the current policy π is also optimal. Thus, any policy satisfying $p^\pi(\mathbf{s}_{t+}) = c \cdot p(\mathbf{s}_t | \mathbf{e}_t = 1)$ is a fixed point of iterated RCE. □

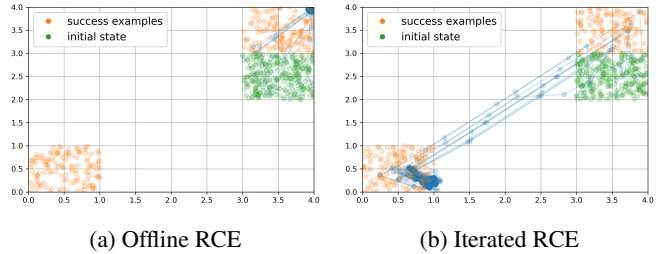


Figure 5. A 2D navigation task with two sets of success states. (Left) When we apply RCE to this task without online data collection, the agent navigates directly toward the closer set of success states. (Right) When we run RCE in an iterated fashion, periodically collecting new transitions using the current policy, the learned policy visits both sets of success states. The behavior of iterated RCE is similar to what we would expect from robust example-based control.

When we are given a discrete set of success examples, the assumption in Eq. 29 is equivalent to assuming that the optimal robust policy spends an equal fraction of its time at each success example.

Lemma C.2. *Assume there exists a policy π such that $p^\pi(\mathbf{s}_{t+}) = p(\mathbf{s}_t \mid \mathbf{e}_t = 1)$. Then the solution to robust example-based control is a fixed point of iterated RCE.*

Proof. As shown in Lemma 4.4, the robust example-based control corresponds to minimizing the squared Hellinger distance, an f -divergence. All f -divergences are minimized when their arguments are equal (if feasible), so the solution to robust example-based control is a policy π satisfying $p^\pi(\mathbf{s}_{t+}) = p(\mathbf{s}_t \mid \mathbf{e}_t = 1)$.

Now, we need to show that such a policy is a fixed point of iterated RCE. If $p^\pi(\mathbf{s}_{t+}) = p(\mathbf{s}_t \mid \mathbf{e}_t = 1)$, then Eq. 3 tells us that $p(\mathbf{e}_t = 1 \mid \mathbf{s}_t)$ is a constant for all states. In this setting, all policies are optimal under our objective (Def. 1), so the current policy π is also optimal. Thus, any policy satisfying $p^\pi(\mathbf{s}_{t+}) = p(\mathbf{s}_t \mid \mathbf{e}_t = 1)$ is a fixed point of iterated RCE. \square

While this result offers some explanation for why iterated RCE might be robust, the result is quite weak. First, the assumption that $p^\pi(\mathbf{s}_{t+}) = p(\mathbf{s}_t \mid \mathbf{e}_t = 1)$ for some policy π is violated in most practical environments, as it would imply that the agent spends every timestep in states that are success examples. Second, this result only examines the fixed points of robust example-based control and iterated RCE, and does not guarantee that these methods will actually converge to this fixed point. We aim to lift these limitations in future work.

D. Connection with Success Classifiers and Success Densities

In this section we show that objective function in prior methods for example-based control implicitly depend on where success examples came from.

Nasiriany (2020) learn a reward function by fitting a density model to success examples, $\hat{p}(s^*) \approx p(\mathbf{s}_t \mid \mathbf{e}_t = 1)$. Using this learned density as a reward function is *not* the same as our approach. Whereas our method implicitly corresponds to the reward function $r(\mathbf{s}_t) = (1 - \gamma)p(\mathbf{e}_t = 1 \mid \mathbf{s}_t)$, the reward function in Nasiriany (2020) corresponds to $\exp r(\mathbf{s}_t) = p(\mathbf{s}_t \mid \mathbf{e}_t = 1) = p(\mathbf{e}_t = 1 \mid \mathbf{s}_t)p_U(\mathbf{s}_t)/p(\mathbf{e}_t = 1)$. The additional $p_U(\mathbf{s}_t)$ term in the (exponentiated) Disco RL reward function biases the policy towards visiting states with high density under the $p_U(\mathbf{s}_t)$ marginal distribution, *regardless of whether those states were actually labeled as success examples*.

In contrast, VICE (Fu et al., 2018b) learns a classifier to distinguish success examples $s^* \sim p(\mathbf{s}_t \mid \mathbf{e}_t = 1)$ from “other” states sampled from $q(\mathbf{s}_t)$. The predicted probability ratio from the Bayes-optimal classifier is

$$\frac{p(\mathbf{s}_t \mid \mathbf{e}_t = 1)}{q_E(\mathbf{s}_t)} = \frac{p(\mathbf{e}_t = 1 \mid \mathbf{s}_t)p_U(\mathbf{s}_t)}{p(\mathbf{e}_t = 1)q(\mathbf{s}_t)}.$$

This term depends on the user’s state distribution $p_U(\mathbf{s}_t)$, so without further assumptions, using this probability ratio as a reward function does not yield a policy that maximizes the future probability of success (Eq. 1). We can recover example-based control if we make the additional assumption that $p_U(\mathbf{s}_t) = q(\mathbf{s}_t)$, an assumption not made explicit in prior work. Even with this additional assumption, VICE differs from RCE by requiring an additional classifier.

In summary, these prior approaches to example-based control rely on auxiliary function approximators and do not solve the example-based control problem (Def. 1) without additional assumptions. In contrast, our approach is simpler and is guaranteed to yield the optimal policy.

E. Experimental Details

E.1. Implementation

This method is straightforward to implement on top of any actor-critic method, such as SAC or TD3, only requiring a few lines of code to be added. The only changes necessary are to (1) sample success in the train step and (2) swap the standard Bellman loss with that in Eq. 10. Unless otherwise noted, all experiments were run with 5 random seeds. When plots in the paper combine the results across seeds, this is done by taking the average.

We based our implementation of RCE off the SAC implementation from TF-Agents (Guadarrama et al., 2018). We modified the critic loss to remove the entropy term and use our loss (Eq. 10) in place of the Bellman loss, modified the TD targets to

use n -step returns with $n = 10$, and modified the actor loss to use a fixed entropy coefficient of $\alpha = 1e - 4$. To implement n -step returns, we replaced the target value of $y = \frac{\gamma w^{(t)}}{\gamma w^{(t)} + 1}$ with $y = \frac{1}{2} \left(\frac{\gamma w^{(t)}}{\gamma w^{(t)} + 1} + \frac{\gamma^{10} w^{(t+10)}}{\gamma^{10} w^{(t+10)} + 1} \right)$. We emphasize that implementing RCE therefore only required modifying a few lines of code. Unless otherwise noted, all hyperparameters were taken from that implementation (version v0.6.0). For the image-based experiments, we used the same architecture from CURL (Srinivas et al., 2020), sharing the image encoder between the actor and classifier. Initial experiments found that using random weights for the image encoder worked at least as well as actually training the weights of the image encoder, while also making training substantially faster. We therefore used a random (untrained) image encoder in all experiments and baselines on the image-based tasks. We used the same hyperparameters for all environments, with the following exception:

- `sawyer_bin_picking`: The SAC implementation in TF-Agents learns two independent Q values and takes the minimum of them when computing the TD target and when updating the policy, as suggested by Fujimoto et al. (2018). However, for this environment we found that the classifier’s predictions were too small, and therefore modified the actor and critic losses to instead take the maximum over the predictions from the two classifiers. We found this substantially improved performance on this task.

E.2. Baselines.

We implemented the SQIL baseline as an ablation to our method. The two differences are (1) using the standard Bellman loss instead of our loss (Eq. 10) and (2) not using n -step returns. We implemented all other baselines on top of the official DAC repository (Kostrikov et al., 2018). For fair comparison with our method, the classifier was only conditioned on the state, not the action. These baselines differed based on the following hyperparameters:

Method name	gradient penalty	discriminator loss	absorbing state wrapper
DAC	10	cross_entropy	yes
AIRL	0	cross_entropy	no
ORIL-PU	0	positive_unlabeled	no
PURL	0	positive_unlabeled_margin	no

Table 1. Classifier-based baselines

The done bit wrapper is the idea discussed in DAC (Kostrikov et al., 2018, Sec. 4.2). The `cross_entropy` loss is the standard cross entropy loss. The `positive_unlabeled` loss is the standard positive-unlabeled loss (Elkan & Noto, 2008); following Zolna et al. (2020, Appendix B, Eq. 5) we used $\eta = 0.5$. The `positive_unlabeled_margin` loss is taken from Xu & Denil (2019, Eq. 9), as are the hyperparameters of $\eta = 0.5, \beta = 0.0$.

E.3. Environments

Our experiments used benchmark manipulation tasks from Metaworld (Jan. 31, 2020) (Yu et al., 2020) and D4RL (Aug. 26, 2020) (Fu et al., 2020; Rajeswaran et al., 2018). Unless otherwise mentioned, we used the default parameters for the environments.

1. `sawyer_drawer_open`: This task is based on the `SawyerDrawerOpenEnv` from Yu et al. (2020). We generated success examples by sampling the drawer Y coordinate from `unif(low=-0.25, high=-0.15)` and moving the gripper to be touching the drawer handle. Episodes were 151 steps long. For evaluation, we used the net distance that the robot opened the drawer (displacement along the negative Y axis) as the reward.
2. `sawyer_push`: This task is based on the `SawyerReachPushPickPlaceEnv` from Yu et al. (2020), using `task_type = 'push'`. We generated success examples by sampling the puck XY position from `unif(low=(0.05, 0.8), high=(0.15, 0.9))` and moving the gripper to be touching the puck. Episodes were 151 steps long. For evaluation, we used the net distance that the puck traveled towards the goal as the reward.
3. `sawyer_lift`: This task is based on the `SawyerReachPushPickPlaceEnv` from Yu et al. (2020), using `task_type = 'reach'`. We generated success examples by sampling the puck Z coordinate from `unif(low=0.08, high=0.12)` and moving the gripper such that the puck was inside the gripper. Episodes were 151 steps long. For evaluation, we used the Z coordinate of the puck at the final time step.

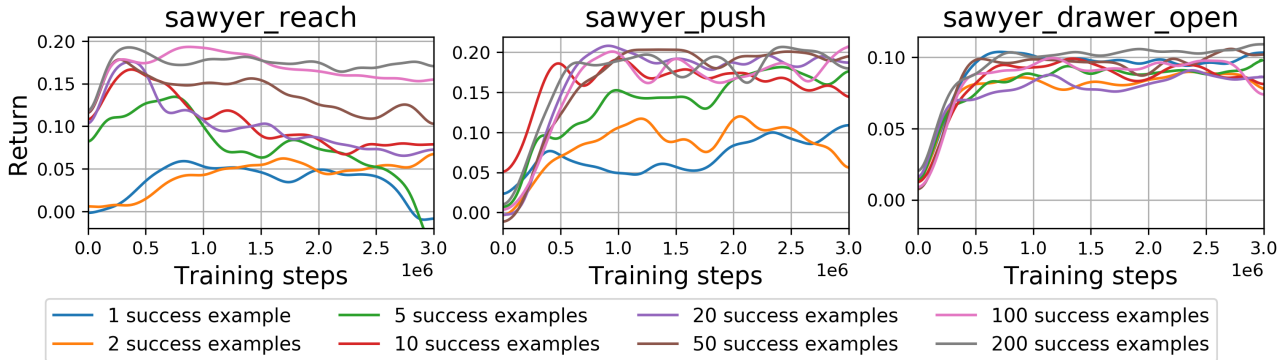


Figure 6. **Number of success examples:** While we used 200 success examples in each experiment in the paper, a later ablation experiment showed that RCE can learn effectively with fewer success examples. We can achieve comparable performance using 100 examples for the sawyer_reach task, 20 examples for the sawyer_push task, and just 1 example for the sawyer_drawer_open task.

4. sawyer_box_close: This task is based on the SawyerBoxCloseEnv from Yu et al. (2020). We generated success examples by positioning the lid on top of the box and positioning the gripper so that the lid handle was inside the gripper. Episodes were 151 steps long. For evaluation, we used the net distance that the lid traveled along the XY plane towards the center of the box.
5. sawyer_bin_picking: This task is based on the SawyerBinPickingEnv from Yu et al. (2020). We generated success examples by randomly positioning the object in the target bin, sampling the XY coordinate from $\text{unif}(\text{low}=(0.06, 0.64), \text{high}=(0.18, 0.76))$ and positioning the gripper so that the object was inside the gripper. Episodes were 151 steps long. For evaluation, we used the net distance that the object traveled along the XY plane towards the center of the target bin.
6. door-human-v0, hammer-human-v0: These tasks are described in (Rajeswaran et al., 2018). We generated success examples by taking a random subset of the last 50 observations from each trajectory of demonstrations provided for these tasks in (Fu et al., 2020). We used the default episode length of 200 for these tasks. For evaluation, we used the default reward functions for these tasks (which are a few orders of magnitude larger than the net-distance rewards used for evaluating the sawyer tasks.).
7. sawyer_reach_random_position_image, sawyer_reach_random_size_image: These image-based reaching tasks are based on the SawyerReachPushPickPlaceEnv task from Yu et al. (2020), using `task_type = 'reach'`. We generated success examples by positioning the gripper at the object. Episodes were 51 steps long. For evaluation, we used the net distance traveled towards the object as the reward. The sawyer_reach_random_position_image modified the environment to initialize each episode by randomly sampling the object position from $\text{unif}(\text{low}=(-0.02, 0.58), \text{high}=(0.02, 0.62))$. The sawyer_reach_random_size_image modified the environment to initialize each episode by randomly resizing the object by sampling a radius and half-height from $\text{unif}(\text{low}=(0.1, 0.005), \text{high}=(0.05, 0.045))$.
8. sawyer_clear_image: This task is based on the SawyerReachPushPickPlaceEnv from Yu et al. (2020), using `task_type = 'push'`. We generated success examples by simply deleting the object from the scene and setting the gripper to a random position drawn from $\text{unif}(\text{low}=(-0.2, 0.4, 0.02), \text{high}=(0.2, 0.8, 0.3))$. For evaluation, we used a reward of 1 if the object was out of sight, as defined by having a Y coordinate less than 0.41 or greater than 0.98.

F. Ablation Experiments and Visualization

We ran three ablation experiments to further understand our method. First, we studied the effect of the number of success examples by varying that value from 1 to 200. We ran each experiment with 5 random seeds, but only plot the mean across seeds to avoid visual clutter. As shown in Fig. 6, performance only decreased substantially when the number of success examples was 20 or lower. Second, we studied the effect of the approximation made in Sec. 3.2, where we sampled actions

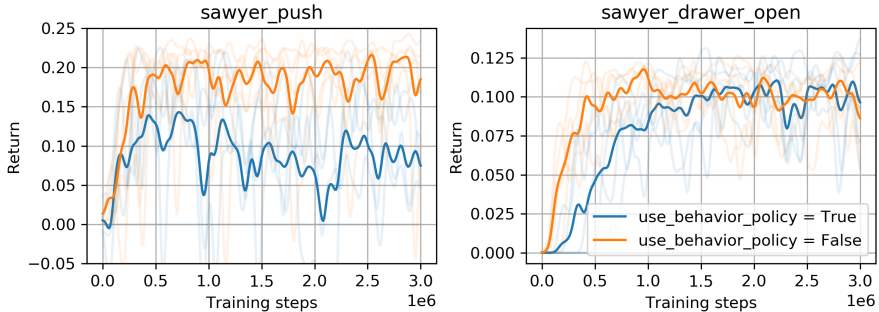


Figure 7. **Actions for success examples:** While our theory suggests to label the success examples with actions from the behavior policy, in most of our experiments we used actions from the current (learned) policy. We compared the performance of these two strategies on the sawyer_push and sawyer_drawer_open tasks, finding that using the current policy did not hurt performance.

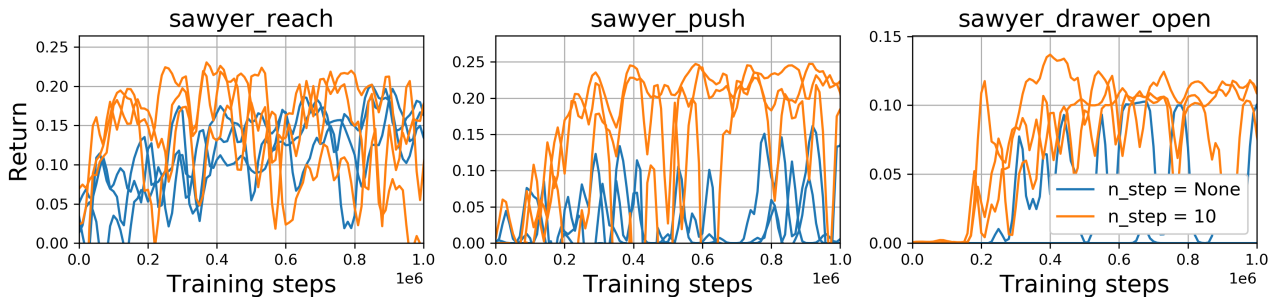


Figure 8. **N-step returns:** We consistently found that using n-step returns improved performance. For all experiments with our method, we used $n = 10$.

for the success examples using our current policy instead of the historical average policy. To do this, we fit a new behavior policy to our replay buffer using behavior cloning, and used this behavior policy to sample actions for the success examples. However, as shown in Fig. 7, we found that simply using our current policy instead of this behavior policy worked at least as well, while also being simpler to implement. Third, we studied the effect of using n-step returns. As shown in Fig. 8, using n-step returns substantially improved performance on the sawyer_push and sawyer_drawer_open tasks, and had a smaller positive effect on the sawyer_reach task. Finally, to better illustrate the mechanics of our method, we ran RCE on a simple 2D navigation task. We then visualized the classifier’s predictions throughout training. As shown in Fig. 9, the classifier’s predictions are initially mostly uniform across all states, but later converge to predict much larger values near the success examples and lower values elsewhere.

G. Failed Experiments

This section describes a number of experiments that we tried that did not work particularly well. We did not include any of these ideas in our final method.

1. **Training the image encoder.** For the image-based experiments, we found that *not* training the image encoder and just using random weights often worked better than actually learning these weights.

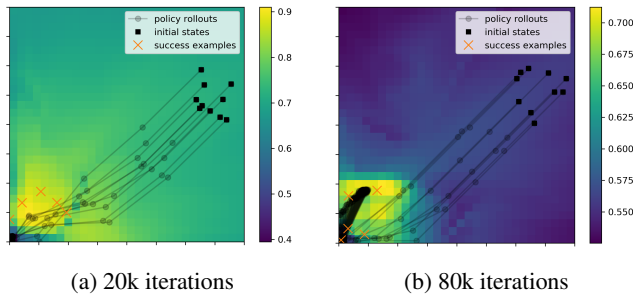


Figure 9. Visualizing the classifier’s predictions and policy rollouts throughout training. To avoid visual clutter, we plot a random subset of the success examples.

2. **Alternative parametrization of the classifier.** By default, our classifier predicts values in the range $C_\theta \in [0, 1]$. However, Eq. 5 says that the classifier’s predicted probability ratio corresponds to

$$p^\pi(\mathbf{e}_{t+} = 1 \mid \mathbf{s}_t, \mathbf{a}_t) = \frac{C_\theta^{(t)}}{1 - C_\theta^{(t)}} \in [0, 1].$$

We therefore expect that a learned classifier should only make predictions in the range $[0, 0.5]$. We experimented by parametrizing the classifier to only output values in $[0, 0.5]$, but found that this led to no noticeable change in performance.

3. **Classifier regularization.** We experimented with regularizing our classifier with input noise, gradient penalties, mixup, weight decay and label smoothing. These techniques yield improvements that were generally small, so we opted to not include any regularization in our final method to keep it simple.
4. **Regularizing the *implicit* reward.** We can invert our Bellman equation (Eq. 12) to extract the reward function that has been implicitly learned by our method:

$$r(\mathbf{s}_t, \mathbf{a}_t) = \frac{C_\theta^{(t)}}{1 - C_\theta^{(t)}} - \gamma \frac{C_\theta^{(t+1)}}{1 - C_\theta^{(t+1)}}.$$

We experimented with regularizing this implicit reward function to be close to zero or within $[0, 1]$, but saw no benefit.

5. **Normalizing w .** We tried normalizing the TD targets w (Eq. 9) to have range $[0, 1]$ by applying a linear transformation (subtracting the min and dividing by the max-min), but found that this substantially hurt performance.
6. **Hyperparameter robustness.** We found that RCE was relatively robust to the learning rate, the discount factor, the Polyak averaging term for target networks, the batch size, the classifier weight initialization, and the activation function.
7. **Imbalanced batch sizes.** Recall that our objective (Eq. 10) uses a very small weight of $(1 - \gamma)$ for the first term. This small weight means that our effective batch size is relatively small. We experimented with changing the composition of each batch to include fewer success examples and more random examples, updating the coefficients for the loss terms such that the overall loss remained the same. While this does increase the effective batch size, we found it had little effect on performance (perhaps because our method is fairly robust to batch size, as noted above).
8. **Optimistic initialization.** We attempted to encourage better exploration by initializing the final layer bias of the classifier so that, at initialization, the classifier would predict $C_\theta = 1$. We saw no improvements from this idea.